FEBS Letters 587 (2013) 2996–3001

FEBS Letters

journal homepage: www.FEBSLetters.org

In silico investigation of PHD-3 specific HIF1-α proline 567 hydroxylation: A new player in the VHL/HIF-1α interaction pathway?

Giovanni Minervini [a], Alessandro Masiero [a], Stefano Moro [b], Silvio C.E. Tosatto [a,*]

[a] Dept. of Biology, University of Padova, Italy
[b] Dept. of Pharmaceutical Sciences, University of Padova, Italy

ARTICLE INFO

Article history:
Received 19 March 2013
Revised 28 June 2013
Accepted 15 July 2013
Available online 22 July 2013

Edited by Robert B. Russell

Keywords:
Molecular dynamic
von Hippel–Lindau
Hypoxia inducible factor 1
Sequence analysis
Structural bioinformatic
Cancer

ABSTRACT

Hypoxia inducible factor 1α (HIF-1α) regulates oxygen homeostasis in the cell through a sensing mechanism involving its hydroxylation and binding to the von Hippel–Lindau (VHL) tumor suppressor. This mechanism is mediated through hydroxylation of HIF-1α proline 564, although in vitro tests have previously shown an alternative hydroxylation at proline 567 by PHD-3. Here, molecular dynamics simulations were used to investigate the structural effect of this alternative hydroxylation. A specific hydrogen bond network rearrangement and improved electrostatic energy for hydroxylated P567 are compatible with an increase in HIF-1α binding affinity. Sequence analysis also confirms P567 to be vastly conserved during evolution, indicating a possible role for this alternative, PHD-3 driven, post translational modification in pVHL–HIF-1α complex formation.

1. Introduction

Hypoxia is a pathological condition commonly present in tissue tumor growth. Hypoxia inducible factor 1α (HIF-1α) is a key transcription factor of oxygen homeostasis regulation in the cell. HIF-1α directly regulates the expression of over 40 important target genes such as vascular endothelial growth factor (VEGF), erythropoietin, glycolytic enzymes, and glucose transporters [1]. The HIF-1α concentration is regulated through ubiquitin-mediated proteolysis, governed by the activity of the von Hippel–Lindau (VHL) tumor suppressor protein (pVHL) [2]. VHL is the key player in VHL syndrome, a dominantly inherited familial cancer syndrome with variable expression and an age-dependent penetrance. It is characterized by a predisposition to develop retinal and central nervous system hemangioblastomas, pheochromocytomas, clear cell renal carcinomas, islet cell tumors of the pancreas, and endolynphatic sac tumors, as well as cysts and cystadenomas in the kidney, pancreas, epididymis, and broad ligament [3,4]. The predisposition to develop this variety of tumors is linked to germline inactivation of VHL. Development of the pathology in VHL disease occurs subsequently to somatic inactivation of the remaining wild-type allele in a susceptible cell [5]. Importantly, sporadic forms of the same tumor types that are common in familial VHL disease display bi-allelic somatic VHL inactivation through a variety of mechanisms, including mutations and hypermethylation. For example, inactivation of VHL has been demonstrated in 70–80% of all sporadic clear cell renal cell carcinomas [6]. pVHL is a multifunctional adapter that interacts with numerous proteins such as ElonginB/C-Cullin2, to form the well characterized VBC degradation complex [7,8], and cytoplasmic microtubules during mitosis [9]. Previous computational work on VHL has mainly concentrated on analyzing the many known pVHL interactions [10] and explaining possible effects of known mutations either empirically [11,12] or with molecular dynamics simulations [13–15].

VBC mediated degradation of HIF-1α under normal oxygen conditions is promoted by oxygen-dependent hydroxylation of P564 and P402 residues operated by members of the HIF-prolyl hydroxylase family (PHDs) [16,17]. A crystal structure of the VBC/HIF-1α complex (1.8 Å) including the HIF-1α recognition mechanism operated by pVHL was solved in 2002 [18]. The protein–protein interaction is mediated by a highly conserved hydrogen bonds network between pVHL residues S111, H115, W117 and the hydroxylated HIF-1α P564. Under pathological conditions, such as tumor growth, lack of oxygen inhibits normal

* Corresponding author. Address: Dept. of Biology, University of Padova, viale G. Colombo 3, 35131 Padova, Italy. Fax: +39 049 827 6260.
E-mail address: silvio.tosatto@unipd.it (S.C.E. Tosatto).

0014-5793/$36.00
http://dx.doi.org/10.1016/j.febslet.2013.07.019

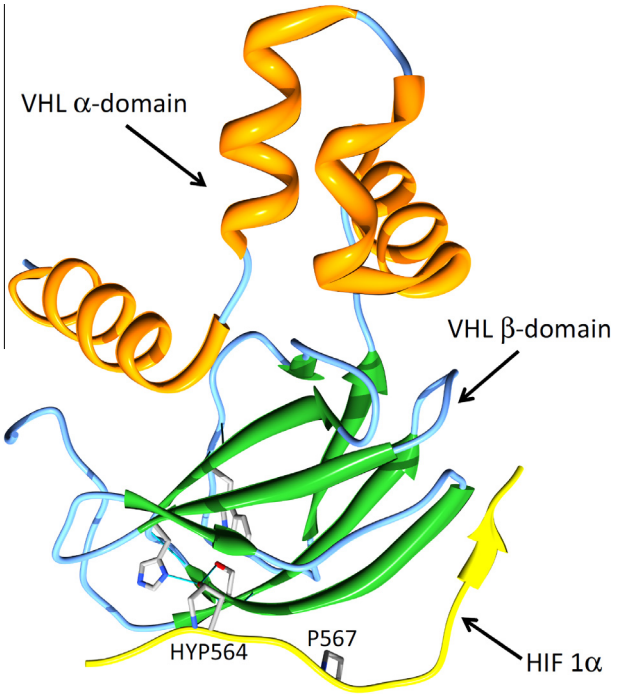

Fig. 1. Overview of the pVHL/HIF-1α complex. Cartoon representation of the crystallographic structure of pVHL in complex with HIF-1α (PDB identifier 1LM8). The pVHL α-domain is shown in orange color, while the pVHL β-domain is in green and HIF-1α peptide in yellow. Hydrogen bonds are shown as thin blue lines. The HYP564 and P567 side chains are shown in sticks and labeled.

PHD activity and results in reduced HIF-1α degradation [19]. Loss of HIF-1α degradation then promotes transcriptional activation of numerous genes, resulting in the commonly observed hypervascularized tumors and cysts observed in VHL patients [20]. The post translational modification introduced by PHD assumes a crucial role in HIF-1α balance and regulation. The HIF-prolyl hydroxylases are a heterogeneous enzyme family composed of three different proteins termed PHD-1 to -3. PHD-3, in particular, appears to be a functionally specialized paralog of the first two enzymes. Smaller, and with a markedly different cellular localization, it was recently demonstrated to also have a different substrate specificity, at least in vitro [21]. While PHD-1 and -2 require a specific target sequence, known as LxxLAP motif [16], PHD-3 seems to be less sequence specific and able to carry out its hydroxylation activity with the only requirement of a proline residue in the linear motif. In 2007, Fedulova and co-workers demonstrated that PHD-3 hydroxylates P567 in HIF-1α [22], which is not LxxLAP motif compliant. In another work, the same residue was also reported to increase the binding affinity of PHD-3 [23]. Both observations suggest the possible existence of an alternative HIF-1α regulation pathway mediated by PHD-3. Here, we used molecular dynamics to investigate the structural effect on the pVHL/HIF-1α binding interface when P567 is hydroxylated. Sequence analysis confirms P567 to be broadly conserved during evolution, further strengthening the idea of an evolutionarily conserved functional mechanism.

2. Methods

2.1. Molecular dynamics simulations

The crystal structure of pVHL solved at 1.8 Å resolution [18] (PDB identifier 1LM8) was used as a starting model, considering chains V (pVHL) and H (HIF-1α peptide). Chains B and C, corresponding to Elongin B and C respectively, were excluded from the simulations as they are distant from the pVHL/HIF-1α interaction site with 40 and 55 Å, respectively and should not have a direct effect on the binding interface interactions of interest for the present work. The pVHL crystal structure also lacks 6 N-terminal and 4 C-terminal residues, which are also not involved in HIF-1α interaction. The protonation state of the protein was adjusted to mimic a pH value of 7.0. All lysine residues were positively charged and histidine residues were modeled as neutral by protonating the Nε2 atom. In particular, H115 was modeled as neutral by protonating the Nδ1 atom as reported in the crystal structure [18]. Aspartate and glutamate residues were considered fully deprotonated. All simulations were carried out with Gromacs [24], using the CHARMM 27 [25] force field. Hydrogen atoms were added to the system by means of the Gromacs pdb2gmx routine. Each run was constituted by a minimization step, 100 ps of NVT (constant number of molecules, volume and temperature) simulation, 100 ps of NPT (constant number of molecules, pressure and temperature) simulation and 50 ns of classical molecular dynamics (MD) simulation. The minimization used a steepest descent algorithm. NVT simulations were performed with no pressure coupling. Temperature was coupled with a modified Berendsen thermostat, to obtain a Maxwell distribution of energies. Temperature was kept at 300 K. NPT simulations were performed with a Parinello-Rahman barostat, at a temperature of 300 K, and the pressure was kept at 1 atm. The solvent box was generated covering a distance of 10 Å from the farthest point of the protein boundaries on each of the three dimensions. The generated box was constituted by $\sim 1.8 \times 10^4$ TIP3p water molecules, and sized 82^3 Å. As HYP is not a standard amino acid, its parameters are not included in standard molecular modeling force fields. A proper set of values, compatible with the CHARMM 27 force field was generated and used for the simulation as follows. The CHARMM force field includes four different contributions, namely bond stretching, angle bending, bond rotation and non-bonded interactions. For the first three we used CHARMM standard values. To obtain partial atomic charges, HYP was examined with the MOPAC AM1 (URL: http://OpenMOPAC.net/) ab initio method. The charges were almost all comparable, with small differences in the CD atom (see Supplementary material), which according to our calculations appears to be slightly positively charged, as it is bound to a peptide nitrogen atom, in agreement with previous AMBER calculations [26]. The charges were implemented in CHARMM27 force field, as previously done for collagen peptides [27,28]. The resulting values are shown in Supplementary Fig. 1. HYP567 was generated keeping the same stereoisomer as HYP564, and both 4-hydroxyl moieties were placed in the (R) conformation. The total system charge was neutralized by one chloride ion. Default CHARMM parameters were used for ions in bulk solution. All systems were caged into periodic boundary condition cells and Particle Mesh Ewald (PME) grids. All MD runs are 50 ns long and performed on a x86 Linux cluster. The average occupancy was 32 cores per run. To confirm the simulation results shown, two different MD runs were used for each analyzed system. The stereochemical quality of the system at frame 0 was confirmed using PROCHECK [29] and TAP [30].

2.2. Electrostatic analysis

Electrostatic interaction energies were derived using APBS [31], which calculates them by splitting the complex into two separate interactors. The transfer free energies are determined from a homogeneous dielectric environment to an inhomogeneous dielectric environment with different bulk and solvent dielectric constants. The difference between the energetic state of the divided interactors with inhomogeneous dielectrics and

the complex with inhomogeneous dielectrics represents the binding energy estimate. The APBS calculations were carried out on the last frame of each run.

2.3. Sequence analysis

A multiple sequence alignment of the HIF-1α sequence surrounding the hydroxylation site was extracted from Pfam [32] family PF11413 to map the evolutionary conservation of residue P567. All Metazoan sequences, covering 327 sequences and 100 species were collected (accessed on 25th June 2013). A sequence logo was built with [33] from this data and overlaid with the experimental HIF-1α peptide structure from PDB identifier 1lm8, chain H [18]. Intrinsic disorder for the HIF-1α sequence was predicted with CSpritz [34].

3. Results

3.1. Molecular dynamics simulations

The pVHL protein is composed of two main domains, termed α- and β-domain, respectively. The α-domain is known to be partially disordered when not involved in interactions with other proteins, while the β-domain is definitely more stable due to the presence of long β-strands (see Fig. 1). To investigate the effect induced by HIF-1α P567 hydroxylation, a 50 ns MD simulation was performed on the pVHL/HIF-1α complex. Four different conditions were postulated and analyzed: hydroxylation of P564 (HYP564), hydroxylation of P567 (HYP567), hydroxylation of both P564 and P567 and the pVHL/HIF-1α complex without post-translational modifications. The unmodified complex was also used as baseline to configure the simulation environment. The variation of the weighted root-mean-square deviations (RMSD) was monitored to investigate the stability of pVHL/HIF-1α interaction. RMSD plots obtained for the four analyzed systems are shown in Fig. 2. The steady RMSD observed for the backbone atoms indicates that the four systems remain stable for the entire simulation time, with the main variations limited to the pVHL α-domain. This result is consistent with the literature [14] and could be considered a reliability check of the MD simulation parameters used. The pVHL/HIF-1α system with no hydroxyproline residues shows a modest but linear RMSD increase during time, suggesting possible major variations over longer simulation times. Analysis of the last MD frame reveals the complex to be compatible with the previously observed crystal structure, revealing small pVHL movements limited to the α-domain. Binding between HIF and pVHL is correctly simulated and consistent with a pseudo β-sheet connection of the HIF linear motif (residues Y565, I566, F572, Q573, L574) and the fourth pVHL β-strand (H110, G106, T105, G104) as previously described [18]. The internal HIF-1α motif region from P566 to D571 shows a stable coil-shaped organization with hydrogen bonds remaining stable during the entire simulation. Similar

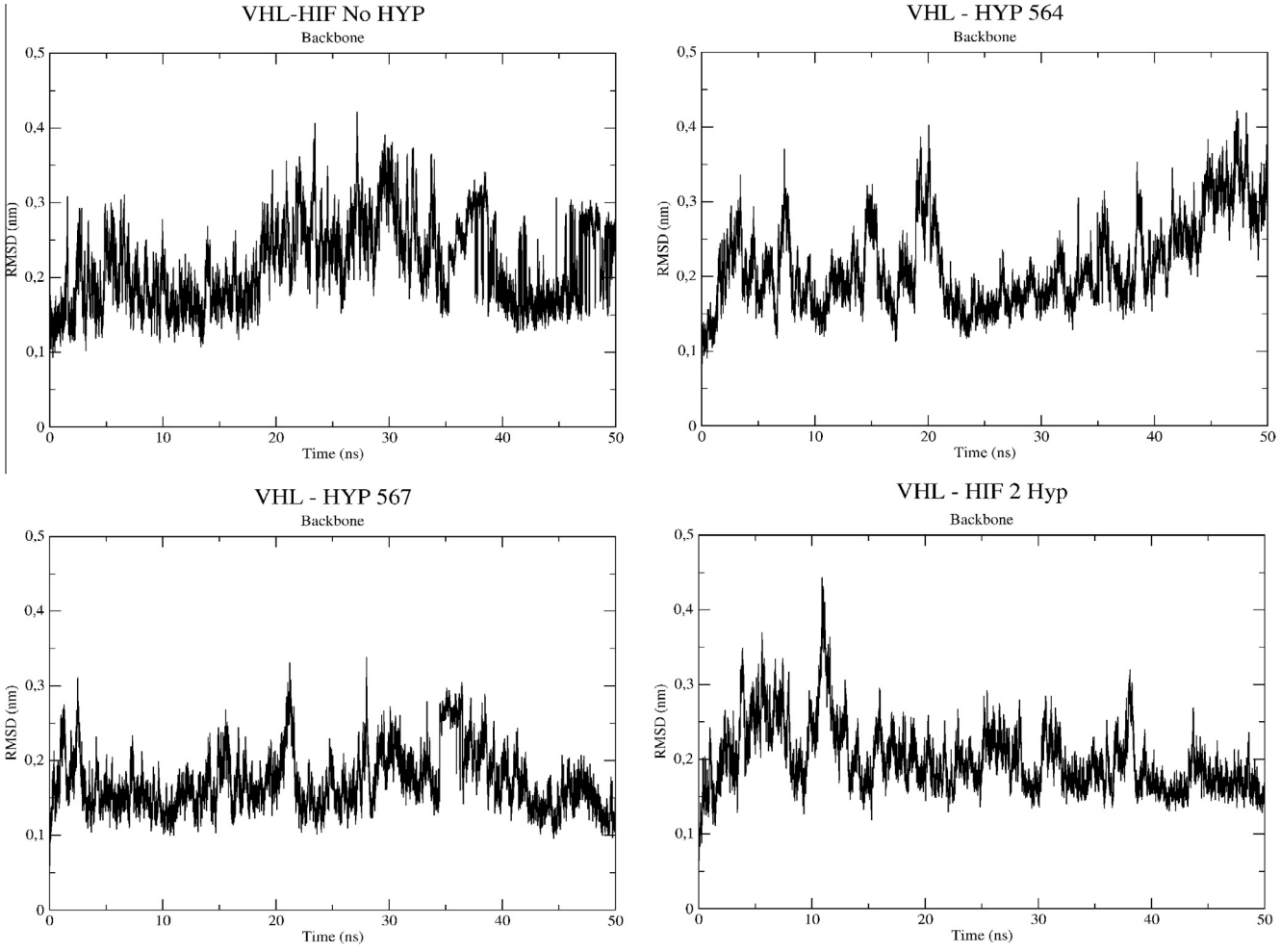

Fig. 2. Weighted RMSD fluctuations of the pVHL/HIF-1α complex backbone over time. The four panels show the results without hydroxyproline (VHL-HIF No HYP), with HYP564 (VHL-HYP 564), with HYP567 (VHL-HYP 567) and with double hydroxylation at HYP564 and HYP567 respectively (VHL-HIF 2 Hyp). The RMSD variation was calculated from their initial position during 50 ns of MD simulation.

results for this region were obtained for all tested systems. pVHL/HIF-1α with HYP564 shows smaller fluctuations in the β-domain, probably due to the stabilizing effect, induced by interactions between pVHL S111, H115, W117 and HYP564 (see Fig. 3). Bigger but not relevant variations (RMSD <0.5 Å) were observed for the α-domain, probably related to the absence of a stabilizing effect usually induced by the ElonginB/C-Cullin2 proteins which were not included in our simulations. The RMSD plot clearly shows how the overall system initially remains stable with little fluctuations. After 40 ns of simulation the RMSD value appears to follow a growing trend (Fig. 2). pVHL/HIF-1α with HYP567 shows less fluctuations, with an estimated average RMSD value around 0.2 Å. Here, we tested if P567 hydroxylation could play a role in pVHL/HIF-1α complex formation. HYP in position 567 is able to promote a new hydrogen bond network localized around HYP567, shown in Fig. 3, involving the pVHL H110, Q73, R108 and HIF-1α D569 residues. This appears to confirm the observation that PHD-3 is able to hydroxylate a proline residue not strictly compliant with the LxxLAP motif. In the double hydroxylated

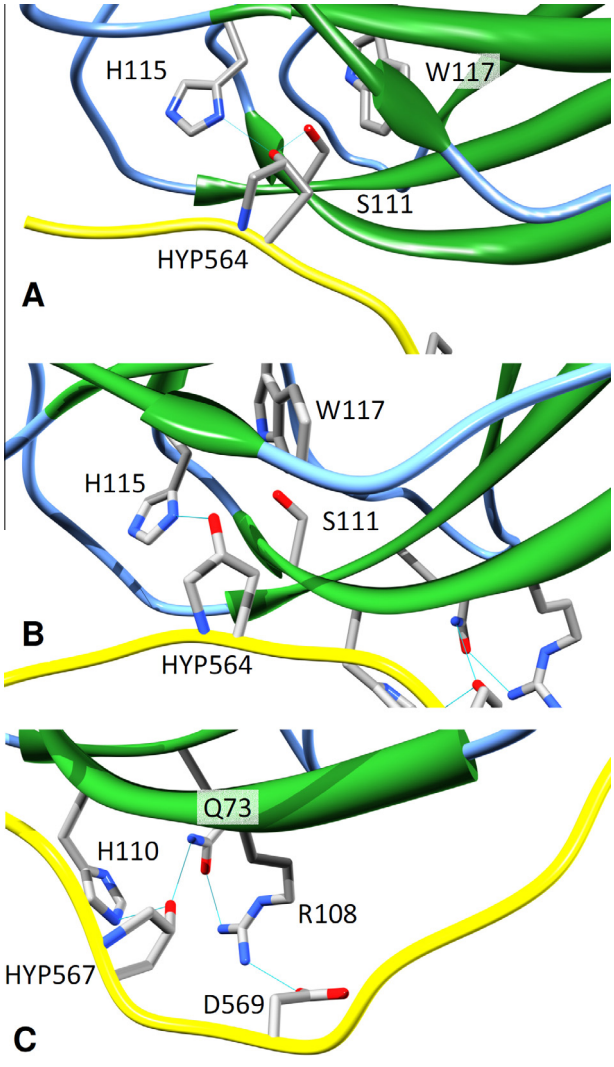

Fig. 3. Hydrogen bond network around the hydroxylated HIF-1α residues. A close-up of the pVHL/HIF-1α complex is shown under different conditions in analogy to Fig. 1. Side chains of involved in the hydrogen bond network of the two hydroxylated prolines are shown as sticks, with thin blue lines representing hydrogen bonds. The three panels are organized as follows: (A) Crystal structure with HYP564. (B) Hydrogen bond network reorganization around residue HYP564 promoted by hydroxylation of PRO567. (C) The putative new hydrogen bond network around HYP567. Notice how hydroxylation of P567 creates novel hydrogen bonds with H110 and Q73, while tilting the positions of S111 and W117.

pVHL/HIF-1α system, the RMSD plot shows an intermediate pattern. For the first 12 ns, the system seems to replicate the previously observed behavior of the non-HYP564, while it and gets closer to the HYP567 behavior for the remaining 38 ns of simulation. A significant spike is visible at 11 ns (Fig. 2) and MD frame analysis reveals a reorganization event of the hydrogen bond network around HYP564 and HYP567. Spikes of similar magnitudes were also noted in RMSD plots for other simulations, but in these cases were related to rearrangement of single side chains involved in the VHL–HIF interaction. In the double hydroxylated system presence of the second hydroxyproline seems to promote an increased distance between HYP564 and pVHL S111 from 2.86 to 4.34 Å, with a consequent partial interruption of the hydrogen bond network. Although a reorientation event of HYP564 and H115 with respect to S111 is visible, the interaction between these residues remains stable during the simulation. The rearrangement of connections seems to be due to the rigidity imposed by the new hydrogen bond network localized around HYP567 and shown in Fig 3. Our simulation results suggest pVHL residues H110, Q73, R108 and HIF-1α D569 to be important to establish the hydrogen bond network around HYP567. Q73 in particular seems to play a key role in establishing this network, although further experimental validation is necessary to confirm its role. Analysis of the pVHL–HIF-1α HYP567 complex trajectory suggests that the P567 modification alone is sufficient to promote the organization of a well structured hydrogen bond network around this residue. Connections with the pVHL H110, Q73, R108 and the HIF-1α D569 residues are apparently formed due to an increased distance between the coil-shaped region and residues on the fourth pVHL β-strand (data not shown). Based on MD simulation results, residue P567 seems important in the complex formation. To investigate the role of single residues in VHL–HIF-1α interaction, a root-mean-square fluctuation (RMSF) analysis was performed, see Supplementary material.

3.2. Control MD simulations

In order to check the pVHL/HIF-1α complex stability two control MD simulations were performed. The first one, derived from sequence analysis, containing the P567S mutant, the second one consisting in P564L and P567L mutants. The MD simulations suggest no destabilization of the pVHL/HIF-1α complex with the P567S substitution, consistent with its presence in a subset of HIF sequences. The P564L and P567L double mutant instead presented a significant destabilization leading to gradual dissociation of the HIF-1a peptide from pVHL. A more detailed analysis, including RMSF, can be found in Supplementary material.

3.3. HIF1-α motif sequence analysis

To reinforce this observation, we made a conservation analysis of the HIF-1α linear motif residues among homologous proteins by selecting all Metazoan HIF sequences in Pfam (see Fig. 4). The sequence logo shows how the HIF-1α linear motif is located in an ordered segment with strong sequence conservation, flanked by charged residues on both sides, inside an otherwise intrinsically disordered region. Such an arrangement is generally indicative of a functional linear motif [35]. In particular, P567 to be conserved in 76% of sequences included in the alignment. The only substitution is serine (24% of sequences), a residue hypothetically compatible with the hydrogen bond network observed around P567 (see Fig. 3). To better understand the role of a serine 567 substitution, we analyzed the sequences presenting the substitution. The mutation seems to be present only in HIF-3α orthologs and a less-characterized subgroup including sweet water fish of the Cypriniformes order. HIF-3α has a different expression pattern from

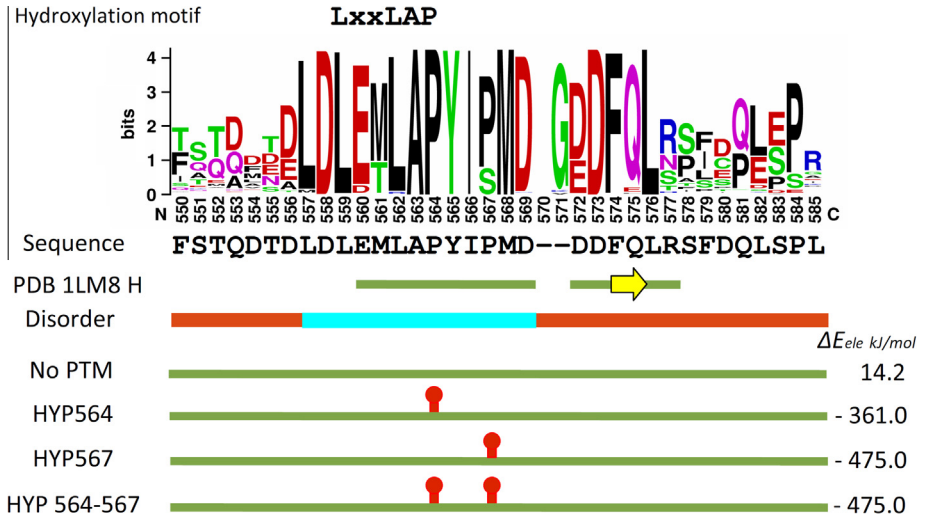

Fig. 4. Overview of the HIF-1α peptide features. The HIF-1α sequence logo surrounding the hydroxylation site is shown with the canonical hydroxylation motif above and the human HIF-1α sequence, features from the crystallographic HIF-1α structure (PDB identifier 1lm8) and predicted disorder below. The secondary structure is shown as a green line for coil and yellow arrow for β-strand. Predicted disorder is shown as a red line and predicted structure in light blue. The bottom part shows a schematic representation of the simulated peptides, with red markers depicting the presence of hydroxylated prolines of the two modeled sites (P564 and P567). The electrostatic component of ΔG calculated with APBS is shown to the right of each simulated peptide.

HIF-1α and -2α [36]. Sweet water ecosystems like shallow lakes or slow rivers during summer are subject to severe oxygen reduction connected with algal bloom phenomena [37]. The existence of an adaptive hypoxia tolerance related to environmental conditions was recently demonstrated for a marine species, the common sole (*Solea solea*) [38] In other words, functional specialization among HIF paralogs and seasonal fluctuations of oxygen concentration may have influenced the evolution of an alternative regulation of the hypoxia response pathway including the S567 mutation.

3.4. In silico electrostatic binding energy calculation

In order to confirm our results with experimental data, putative electrostatic ΔG values were calculated with APBS [31] (see Fig. 4), which evaluates energetic states calculating the difference between the solvated unbound interactors and the solvated complex. The values obtained were compared with previously reported experimental values, where the complex containing HYP564 was reported to have $\Delta G = -9.1 \pm 0.05$ kcal/mol (-38.07 kJ/mol), while no interactions could be detected by the authors on the non-hydroxylated HYP564 complex [18]. According to APBS, the electrostatic ΔG contribution of HYP564 to the complex is -371 kJ/mol, which is consistent with the reported ΔG trend. Repulsive forces seem to appear in the tested non-hydroxylated complex, with a positive electrostatic contribution of 14.2 kJ/mol, consistent with [18]. Based upon these consistent results, electrostatic contributions were calculated with APBS for all complexes. The resulting putative electrostatic contribution of the HYP564/HYP567 complex was -457.5 kJ/mol. The HYP567 complex showed a very similar putative value of -457.3 kJ/mol. Given the in silico nature of the results, we cannot exclude other interpretations or conclusions except that a set of residues present on pVHL is compatible with a post translational modification of both P564 and P567 residues.

4. Discussion

In this work we presented results obtained from MD simulations of the pVHL/HIF-1α complex. Four different hydroxylation patterns (and two controls) were simulated for the proline residues present on a small linear motif of HIF-1α known to interact with pVHL. The simulation started from an observation of Fedulova et al. [22] that PHD-3, a member of human PHD family, hydroxylates the P567 residue not included in the canonical LxxLAP motif usually required by PHD enzymes. PHD-3 differs from other PHD family members by size, cellular localization and target specificity [20]. Here, we tested the structural compatibility of P567 hydroxylation through MD simulations of the effect of this non-conventional hydroxylation on the interaction interface between pVHL and the HIF-1α linear motif. Our results suggest that a previously not described reorganization of hydrogen bond network between pVHL and HIF-1α appears around the HIF-1α P567 linear motif when hydroxylated. Recently, Jaakkola and coworkers [39] demonstrated involvement of PHD-3 in apoptotic events under normoxia, apparently related to an over-saturation of the proteosomal degradation system connected with massive protein aggregation. They also demonstrated a massive transcription induction of PHD-3 mRNA promoted by HIF-1α [23]. Again, their work demonstrates how PHD-3 activity is maximal when oxygen concentration is restored after strong hypoxia events, probably co-occurring with PHD-1 and -2 reactivation. Our results suggest that the reorganization of the hydrogen bond network also appears when both HYP564 and HYP567 are present. This scenario is consistent with two distinct post translational modifications due to the subsequent activity of two different PHD enzymes. On the other hand, due to the massive expression of PHD-3 during hypoxia, it is also possible to imagine that double hydroxylation is the result of a higher intracellular concentration of PHD-3. The latter is also known to be actively expressed, under normal conditions, only in heart and brain tissues [39,21,40]. Considering our results in context of this evidence, it is easy to speculate that they could indicate an alternative regulation pathway trigged by the PHD-3 enzyme. In other words, we can imagine that hydroxylation of P567 could act as a reinforcement of the ubiquitin–proteasome degradation pathway evolving in highly specialized tissues, which are very sensible to oxygen variation. While this evidence is suggestive, we cannot assume that the obtained computational results are exclusively connected with PHD-3 activity and more complex scenarios where different PHDs act in concert cannot be excluded. Furthermore, data presented in this work suffers from limits and approximations inherent in computational techniques. Despite the apparently good results obtained with 50 ns MD simulations, we cannot exclude complex dissociation on longer

timescales. Performing micro or millisecond simulations may provide different outcomes, but is still computationally too expensive to be feasible. Finally, understanding the biological role and relevance of the results presented on the etiopathogenesis of VHL disease will require experimental confirmation, as it is beyond the possibility of the in silico techniques used.

Acknowledgements

This work was supported by AIRC Grant MFAG 12740 to S.T. G.M. is an AIRC research fellow.

Appendix A. Supplementary data

Supplementary data associated with this article can be found, in the online version, at http://dx.doi.org/10.1016/j.febslet.2013.07.019.

References

[1] Semenza, G.L. (1999) Regulation of mammalian O2 homeostasis by hypoxia-inducible factor 1. Annu. Rev. Cell Dev. Biol. 15, 551–578.
[2] Lonser, R.R., Glenn, G.M., Walther, M., Chew, E.Y., Libutti, S.K., Linehan, W.M. and Oldfield, E.H. (2003) Von Hippel–Lindau disease. Lancet 361, 2059–2067.
[3] Gnarra, J.R., Tory, K., Weng, Y., Schmidt, L., Wei, M.H., Li, H., Latif, F., Liu, S., Chen, F. and Duh, F.M. (1994) Mutations of the VHL tumour suppressor gene in renal carcinoma. Nat. Genet. 7, 85–90.
[4] Latif, F., Tory, K., Gnarra, J., Yao, M., Duh, F.M., Orcutt, M.L., Stackhouse, T., Kuzmin, I., Modi, W. and Geil, L. (1993) Identification of the von Hippel–Lindau disease tumor suppressor gene. Science 260, 1317–1320.
[5] Vortmeyer, A.O., Huang, S.C., Pack, S.D., Koch, C.A., Lubensky, I.A., Oldfield, E.H. and Zhuang, Z. (2002) Somatic point mutation of the wild-type allele detected in tumors of patients with VHL germline deletion. Oncogene 21, 1167–1170.
[6] Nyhan, M.J., O'Sullivan, G.C. and McKenna, S.L. (2008) Role of the VHL (von Hippel–Lindau) gene in renal cancer: a multifunctional tumour suppressor. Biochem. Soc. Trans. 36, 472–478.
[7] Feldman, D.E., Thulasiraman, V., Ferreyra, R.G. and Frydman, J. (1999) Formation of the VHL-elongin BC tumor suppressor complex is mediated by the chaperonin TRiC. Mol. Cell 4, 1051–1061.
[8] Melville, M.W., McClellan, A.J., Meyer, A.S., Darveau, A. and Frydman, J. (2003) The Hsp70 and TRiC/CCT chaperone systems cooperate in vivo to assemble the von Hippel–Lindau tumor suppressor complex. Mol. Cell. Biol. 23, 3141–3151.
[9] Thoma, C.R., Toso, A., Gutbrodt, K.L., Reggi, S.P., Frew, I.J., Schraml, P., Hergovich, A., Moch, H., Meraldi, P. and Krek, W. (2009) VHL loss causes spindle misorientation and chromosome instability. Nat. Cell Biol. 11, 994–1001.
[10] Leonardi, E., Murgia, A. and Tosatto, S.C.E. (2009) Adding structural information to the von Hippel–Lindau (VHL) tumor suppressor interaction network. FEBS Lett. 583, 3704–3710.
[11] Leonardi, E., Martella, M., Tosatto, S.C.E. and Murgia, A. (2011) Identification and in silico analysis of novel von Hippel–Lindau (VHL) gene variants from a large population. Ann. Hum. Genet. 75, 483–496.
[12] Forman, J.R., Worth, C.L., Bickerton, G.R.J., Eisen, T.G. and Blundell, T.L. (2009) Structural bioinformatics mutation analysis reveals genotype-phenotype correlations in von Hippel–Lindau disease and suggests molecular mechanisms of tumorigenesis. Proteins 77, 84–96.
[13] Limaverde-Sousa, G., Barreto E de, A., Ferreira, C.G. and Casali-da-Rocha, R.C. (2013) Simulation of the mutation F76del on the von Hippel–Lindau tumor suppressor protein: mechanism of the disease and implications for drug development. Proteins 81, 349–363.
[14] Domene, C. and Illingworth, C.J.R. (2012) Effects of point mutations in pVHL on the binding of HIF-1α. Proteins 80, 733–746.
[15] Liu, J. and Nussinov, R. (2008) Allosteric effects in the marginally stable von Hippel–Lindau tumor suppressor protein and allostery-based rescue mutant design. Proc. Natl. Acad. Sci. USA 105, 901–906.
[16] Ivan, M., Kondo, K., Yang, H., Kim, W., Valiando, J., Ohh, M., Salic, A., Asara, J.M., Lane, W.S. and Kaelin Jr., W.G. (2001) HIFalpha targeted for VHL-mediated destruction by proline hydroxylation: implications for O2 sensing. Science 292, 464–468.
[17] Epstein, A.C., Gleadle, J.M., McNeill, L.A., Hewitson, K.S., O'Rourke, J., Mole, D.R., Mukherji, M., Metzen, E., Wilson, M.I., Dhanda, A., Tian, Y.M., Masson, N., Hamilton, D.L., Jaakkola, P., Barstead, R., Hodgkin, J., Maxwell, P.H., Pugh, C.W., Schofield, C.J. and Ratcliffe, P.J. (2001) *C. elegans* EGL-9 and mammalian homologs define a family of dioxygenases that regulate HIF by prolyl hydroxylation. Cell 107, 43–54.
[18] Min, J.-H., Yang, H., Ivan, M., Gertler, F., Kaelin Jr., W.G. and Pavletich, N.P. (2002) Structure of an HIF-1α–pVHL complex: hydroxyproline recognition in signaling. Science 296, 1886–1889.
[19] McNeill, L.A., Hewitson, K.S., Gleadle, J.M., Horsfall, L.E., Oldham, N.J., Maxwell, P.H., Pugh, C.W., Ratcliffe, P.J. and Schofield, C.J. (2002) The use of dioxygen by HIF prolyl hydroxylase (PHD1). Bioorg. Med. Chem. Lett. 12, 1547–1550.
[20] Taylor, S.R., Singh, J., Sagoo, M.S. and Lightman, S.L. (2012) Clinical and molecular features associated with cystic visceral lesions in von hippel–lindau disease. Open Ophthalmol. J. 6, 83–85.
[21] Hirsilä, M., Koivunen, P., Günzler, V., Kivirikko, K.I. and Myllyharju, J. (2003) Characterization of the human prolyl 4-hydroxylases that modify the hypoxia-inducible factor. J. Biol. Chem. 278, 30772–30780.
[22] Fedulova, N., Hanrieder, J., Bergquist, J. and Emrén, L.O. (2007) Expression and purification of catalytically active human PHD3 in *Escherichia coli*. Protein Expr. Purif. 54, 1–10.
[23] Pescador, N., Cuevas, Y., Naranjo, S., Alcaide, M., Villar, D., Landázuri, M.O. and Del Peso, L. (2005) Identification of a functional hypoxia-responsive element that regulates the expression of the egl nine homologue 3 (egln3/phd3) gene. Biochem. J. 390, 189–197.
[24] Hess, B., Kutzner, C., van der Spoel, D. and Lindahl, E. (2008) GROMACS 4: algorithms for highly efficient, load-balanced, and scalable molecular simulation. J. Chem. Theory Comput. 4, 435–447.
[25] MacKerell, Bashford.D., Bellott, Dunbrack., Evanseck, J.D., Field, M.J., Fischer, S., Gao, J., Guo, H., Ha, S., Joseph-McCarthy, D., Kuchnir, L., Kuczera, K., Lau, F.T.K., Mattos, C., Michnick, S., Ngo, T., Nguyen, D.T., Prodhom, B., Reiher, W.E., Roux, B., Schlenkrich, M., Smith, J.C., Stote, R., Straub, J., Watanabe, M., Wiórkiewicz-Kuczera, J., Yin, D. and Karplus, M. (1998) All-atom empirical potential for molecular modeling and dynamics studies of proteins. J. Phys. Chem. B 102, 3586–3616.
[26] Park, S., Radmer, R.J., Klein, T.E. and Pande, V.S. (2005) A new set of molecular mechanics parameters for hydroxyproline and its use in molecular dynamics simulations of collagen-like peptides. J. Comput. Chem. 26, 1612–1616.
[27] Chang, S.-W., Flynn, B.P., Ruberti, J.W. and Buehler, M.J. (2012) Molecular mechanism of force induced stabilization of collagen against enzymatic breakdown. Biomaterials 33, 3852–3859.
[28] In 't Veld, P.J. and Stevens, M.J. (2008) Simulation of the mechanical strength of a single collagen molecule. Biophys. J. 95, 33–39.
[29] Laskowski, R.A., MacArthur, M.W., Moss, D.S. and Thornton, J.M. (1993) PROCHECK: a program to check the stereochemical quality of protein structures. J. Appl. Crystallogr. 26, 283–291.
[30] Tosatto, S.C.E. and Battistutta, R. (2007) TAP score: torsion angle propensity normalization applied to local protein structure evaluation. BMC Bioinformatics 8, 155.
[31] Baker, N.A., Sept, D., Joseph, S., Holst, M.J. and McCammon, J.A. (2001) Electrostatics of nanosystems: application to microtubules and the ribosome. Proc. Natl. Acad. Sci. USA 98, 10037–10041.
[32] Punta, M., Coggill, P.C., Eberhardt, R.Y., Mistry, J., Tate, J., Boursnell, C., Pang, N., Forslund, K., Ceric, G., Clements, J., Heger, A., Holm, L., Sonnhammer, E.L.L., Eddy, S.R., Bateman, A. and Finn, R.D. (2012) The Pfam protein families database. Nucleic Acids Res. 40, D290–301.
[33] Crooks, G.E., Hon, G., Chandonia, J.-M. and Brenner, S.E. (2004) WebLogo: a sequence logo generator. Genome Res. 14, 1188–1190.
[34] Walsh, I., Martin, A.J.M., Di Domenico, T., Vullo, A., Pollastri, G. and Tosatto, S.C.E. (2011) CSpritz: accurate prediction of protein disorder segments with annotation for homology, secondary structure and linear motifs. Nucleic Acids Res. 39, W190–196.
[35] Davey, N.E., Van Roey, K., Weatheritt, R.J., Toedt, G., Uyar, B., Altenberg, B., Budd, A., Diella, F., Dinkel, H. and Gibson, T.J. (2012) Attributes of short linear motifs. Mol. BioSyst. 8, 268–281.
[36] Hara, S., Hamada, J., Kobayashi, C., Kondo, Y. and Imura, N. (2001) Expression and characterization of hypoxia-inducible factor (HIF)-3alpha in human kidney: suppression of HIF-mediated gene expression by HIF-3alpha. Biochem. Biophys. Res. Commun. 287, 808–813.
[37] Hudnell, H.K., Dortch, Q. and Zenick, H. (2008) An overview of the interagency, International Symposium on Cyanobacterial Harmful Algal Blooms (ISOC-HAB): advancing the scientific understanding of freshwater harmful algal blooms. Adv. Exp. Med. Biol. 619, 1–16.
[38] Zambonino-Infante, J.L., Claireaux, G., Ernande, B., Jolivet, A., Quazuguel, P., Sévère, A., Huelvan, C. and Mazurais, D. (2013) Hypoxia tolerance of common sole juveniles depends on dietary regime and temperature at the larval stage: evidence for environmental conditioning. Proc. Biol. Sci. 280, 20123022.
[39] Rantanen, K., Pursiheimo, J., Högel, H., Himanen, V., Metzen, E. and Jaakkola, P.M. (2008) Prolyl hydroxylase PHD3 activates oxygen-dependent protein aggregation. Mol. Biol. Cell 19, 2231–2240.
[40] Cioffi, C.L., Liu, X.Q., Kosinski, P.A., Garay, M. and Bowen, B.R. (2003) Differential regulation of HIF-1 alpha prolyl-4-hydroxylase genes by hypoxia in human cardiovascular cells. Biochem. Biophys. Res. Commun. 303, 947–953.